



## Article

# Morphological and Functional Alterations in Zebrafish (*Danio rerio*) Liver after Exposure to Two Ecologically Relevant Concentrations of Lead

Rachele Macirella <sup>1,†</sup> , Vittoria Curcio <sup>1,†</sup>, Abdalmoiz I. M. Ahmed <sup>1</sup>, Federica Talarico <sup>2</sup>, Settimio Sesti <sup>1</sup>, Enrique Paravani <sup>3</sup>, Lucia Odetti <sup>4</sup>, Marcello Mezzasalma <sup>1</sup> and Elvira Brunelli <sup>1,\*</sup> 

- <sup>1</sup> Department of Biology, Ecology and Earth Science, University of Calabria, Via P. Bucci 4/B, 87036 Rende, Italy; rachele.macirella@unical.it (R.M.); vittoria.curcio@unical.it (V.C.); abdalmoiz.ahmed@unical.it (A.I.M.A.); settimio.sesti@unical.it (S.S.); marcello.mezzasalma@unical.it (M.M.)
- <sup>2</sup> Natural History Museum and Botanical Garden, University of Calabria, 87036 Rende, Italy; federica.talarico@unical.it
- <sup>3</sup> Facultad de Ingeniería, Universidad Nacional de Entre Ríos, Ruta 11, Oro Verde 3101, Argentina; eparavani@ingenieria.uner.edu.ar
- <sup>4</sup> Cát. Toxicol. y Bioq. Legal, FBCB-UNL, Ciudad Universitaria, Paraje El Pozo S/N, Santa Fe 3000, Argentina; luodetti@gmail.com
- \* Correspondence: elvira.brunelli@unical.it; Tel.: +39-0984-492-996
- † These authors contributed equally to this work.



**Citation:** Macirella, R.; Curcio, V.; Ahmed, A.I.M.; Talarico, F.; Sesti, S.; Paravani, E.; Odetti, L.; Mezzasalma, M.; Brunelli, E. Morphological and Functional Alterations in Zebrafish (*Danio rerio*) Liver after Exposure to Two Ecologically Relevant Concentrations of Lead. *Fishes* **2023**, *8*, 342. <https://doi.org/10.3390/fishes8070342>

Academic Editors: Carmelo Iaria, Fabiano Capparucci and Roberta Pecoraro

Received: 24 May 2023  
Revised: 22 June 2023  
Accepted: 23 June 2023  
Published: 28 June 2023



**Copyright:** © 2023 by the authors. Licensee MDPI, Basel, Switzerland. This article is an open access article distributed under the terms and conditions of the Creative Commons Attribution (CC BY) license (<https://creativecommons.org/licenses/by/4.0/>).

**Abstract:** Lead (Pb) is a non-essential, highly toxic, and persistent element widely recognized as one of the most concerning pollutants. It is listed on the Priority List of Hazardous Substances. Widespread environmental contamination from Pb is a serious issue for human health and wildlife. In fish, Pb mainly accumulates in the liver, which is a key component for metal detoxification and excretion processes. In this study, we investigated, for the first time, the morphological and functional injuries induced in zebrafish (*Danio rerio*) liver by two very low and environmentally relevant concentrations of Pb (2.5 and 5 µg/L) after 48, 96, and 192 h of exposure. We observed significant histological alterations in all the exposed samples, and it was demonstrated that the extent of injuries increased with dose and exposure time. The most common modifications observed were congestion of blood vessels and sinusoids, cytoplasmic vacuolizations, parenchyma dyschromia, and macrophage proliferation. Pb administration also resulted in a significant increase in lipid content and the upregulation of key genes that are involved in metal detoxification (*mtf1*) and the defensive response against oxidative stress (*sod1* and *cat*). We show that even very low doses of Pb can disrupt liver morphology and function.

**Keywords:** Pb; liver; molecular biomarkers; histological biomarkers; MTs; SOD; CAT

**Key Contribution:** Most of the information on Pb toxicity in fish comes from studies on high Pb concentrations that are not representative of naturally occurring contamination events. Environmentally relevant concentrations of Pb doses induce severe morphological alterations in zebrafish liver. Pb exposure induces a significant upregulation of antioxidant enzymes and the biosynthesis of MTs.

## 1. Introduction

Heavy metals are a major concern for terrestrial and aquatic ecosystems because of their negative effects (even at very low concentrations), their nondegradable nature, their high capacity for bioaccumulation, and their long-term persistence—making them one of the main global environmental problems of the 21st century [1–3]. Some heavy metals have been classified in terms of biological function as beneficial or essential for living organisms, while others—such as lead (Pb), cadmium (Cd), mercury (Hg), and arsenic

(As)—are considered to be non-threshold micropollutants, which are able to induce toxic effects in living organisms [4–7].

Pb is a highly toxic and non-biodegradable heavy metal listed in the Priority List of Hazardous Substances released by the Agency for Toxic Substances and Disease Registry (ATSDR) [8,9]. Although Pb is naturally occurring in the environment, its unregulated use in a number of human activities (e.g., mining and agriculture activities, paint pigment production) has resulted in an increase in its levels in all environmental compartments, causing great concern for both humans and wildlife [10]. Lead pollution of the aquatic environment occurs through agricultural, domestic, and industrial wastewater discharges, thus exerting a wide range of toxic effects on aquatic biota, including fish [11]. Fish play a prominent role in the functioning and balance of aquatic ecosystems [12], and they are particularly sensitive to environmental pollutants [13–15]; thus, they are good indicators of water quality.

Fish assimilate Pb through direct ingestion (i.e., in food and water), ion exchange across lipophilic membranes (e.g., the gills), or adsorption across specific tissue and membrane surfaces [3]. In fish, numerous detrimental effects induced by Pb have been reported, including genotoxicity [16], oxidative stress induction [17–20], change in the activities of immune-related enzymes and genes [8,21,22], and histological changes in some tissues and organs [16,23–25].

Given its role in metal detoxification and excretion, the liver is a target organ for Pb [21,26]. In freshwater species, waterborne Pb mainly enters through the gills, reaching the liver via the circulatory system [26]. Therefore, the liver has been identified as the main target for Pb accumulation in fish [23,27,28], and the noxious effects induced in this complex organ have been investigated in several species. A systematic review of the literature provides plenty of evidence of the adverse effects induced in the liver, including a modification of liver enzyme activity [29], the occurrence of metabolic disorders [30], and alterations in liver morphology [31–34]. However, all of these studies refer to high Pb concentrations, and there is a lack of knowledge on the effects of Pb at environmentally relevant concentrations [35,36].

It must be emphasized that fish exposed to very low concentrations of Pb may not show obvious signs of pathology, but the subtle morphological and functional alterations induced by the metal can reduce the health of individuals with important and dramatic repercussions at the population level.

Since the 1980s, *Danio rerio* has been used in a broad spectrum of research fields due to its small body size, short reproductive cycle, easy husbandry, and high homology to the human genome. All of these studies provide a powerful basis for using zebrafish as a model organism for aquatic ecotoxicology [37,38]. It is surprising that a very limited number of studies have investigated the hepatotoxic effects of Pb in zebrafish liver; so far, only three studies are available focusing on the induction of metabolic disorders, oxidative stress [39,40], and morphological alterations following chronic exposure to high Pb concentrations (60 mg/L) [41].

To fill the knowledge gap on Pb hepatotoxicity in fish, we here evaluated, for the first time, the effects induced in zebrafish liver by two very low and environmentally relevant concentrations of Pb (2.5 and 5 µg/L) after 48, 96, and 192 h of exposure. The tested doses were selected based on Pb concentrations found in aquatic environments worldwide and, particularly, in the range of Pb concentrations reported from surface waters; therefore, our results also support the implementation of risk assessment protocols [3,35].

Given the general paucity of information about morphological and functional injuries induced by Pb in fish liver, we first assessed the histological alterations, which are widely recognized as the best tool for assessing the effects of chemical contaminants, including heavy metals [42]. Moreover, to allow a more reliable and objective comparison between the experimental groups, we applied a semi-quantitative method to evaluate the severity of the histological changes.

Since histopathological lesions represent an integration of the effects of prior biochemical and physiological perturbations [43], we next analyzed the modulations of some of the genes involved in (i) metal detoxification (metallothionein, *mtf1*) and (ii) oxidative stress defense (i.e., superoxide dismutase-*sod1* and catalase-*cat*) to better clarify the molecular mechanisms underlying Pb hepatotoxicity.

Metallothioneins (MTs) are low-molecular-weight proteins responsible for metal binding, and they are effective in non-essential metal detoxification and protection from oxidative stress processes [44]. The biosynthesis of MTs in fish is induced by a variety of metals, including Pb; thus, it is an excellent biomarker of exposure to metals [45,46].

Pb toxicity in the liver can be mediated via different mechanisms, but the most common response in both fish and mammalian models is the imbalance between reactive oxygen species (ROS) production and the removal of such molecules [47]. The cells counteract ROS overproduction by the induction of antioxidant molecules, which may be either enzymatic (e.g., catalase and superoxide dismutase) or non-enzymatic (e.g., glutathione). Antioxidant responses have been demonstrated in several fish species exposed to Pb, thus supporting the role of such molecules as biomarkers of the oxidative stress induced by heavy metals [21,48–50].

To the best of our knowledge, this is the first study documenting the morphological, morphometric, and functional alterations of low Pb concentrations in fish liver. Our results, providing new insights into lead-induced hepatotoxicity, also contribute to a better understanding of the risk posed by heavy metals to wildlife species under a realistic exposure scenario.

## 2. Materials and Methods

### 2.1. Fish Maintenance

A total of 70 individuals of both sexes (length  $3.5 \pm 0.5$  cm and weight  $0.43 \pm 0.06$  g) were obtained from a local fish retailer. For two weeks, the fish were acclimatized under controlled conditions in aquaria filled with dechlorinated tap water (temperature =  $26 \pm 0.5$  °C, pH = 7.3, conductivity = 300  $\mu\text{S}/\text{cm}$ , dissolved oxygen =  $8 \pm 1$  mg/L, hardness = 100 mg/L  $\text{CaCO}_3$ , and 14:10 light regime). During the acclimatization period, half of the water (50%) was renewed daily, and the fish were fed daily with commercial fish food.

### 2.2. Exposure Conditions

To obtain the two nominal concentrations of 2.5  $\mu\text{g}/\text{L}$  (low concentration) and 5  $\mu\text{g}/\text{L}$  (high concentration), a stock solution (1000  $\mu\text{g}/\text{L}$ ) of lead acetate was prepared in distilled water ( $\text{Pb}(\text{CH}_3\text{CO}_2)_2 \cdot 3\text{H}_2\text{O}$ , Sigma-Aldrich Chemical Co., St. Louis, MO, USA); then, an adequate amount was diluted in dechlorinated water.

To determine the Pb concentrations in the water samples, an Elan DRC-e inductively Coupled Plasma–Mass Spectrometry (ICP–MS) (PerkinElmer SCIEX, Woodbridge, ON, Canada) was used. Samples were diluted in ultrapure nitric acid (500  $\mu\text{L}$ ) and then introduced into the instrument system with a PerkinElmer AS-93 plus autosampler and a cross-flow nebulizer with a Scott-type spray chamber. Quantitative analysis was performed by constructing the calibration curve for the lead on five different plasma mass spectrometry units (calibration range of 0.1–50 g/L). The analytical verification of the actual concentrations was performed throughout the experiment (starting from time 0 every 24 h) (Table S1). No evident variation was recorded, and such a result is in agreement with the data from previous studies ([25] and the references therein).

The two selected concentrations corresponded to 0.00146% and 0.00292% of the median lethal concentration at 96 h ( $\text{LC}_{50_{96\text{h}}}$ ) for adult zebrafish, respectively [39]. Moreover, both doses were selected through considering the pre-existing data on the worldwide concentration of Pb in surface water and can be considered very low and environmentally realistic [3,35].

Fish were exposed to the low or the high Pb dose for 48, 96, and 192 h, resulting in 6 experimental groups ( $n = 10$ ). The control group ( $n = 10$ ) was maintained in aquaria filled with dechlorinated tap water.

During the experiment, temperature, pH, conductivity, dissolved oxygen, hardness, and photoperiods were monitored daily and kept constant, as is described for the acclimatization period. Fish were fed on alternate days, and food waste and debris were removed daily using a fine mesh.

After 48, 96, and 192 h, the fish were immersed in an anesthetic water bath containing ethyl 3-aminobenzoate methanesulfonate (20 mg/L MS 222, Sandoz, Sigma-Aldrich, St. Louis, MO, USA), and the liver was rapidly dissected and processed for subsequent analyses as reported below. For each experimental unit, including the control, two replicates were conducted. The use of animals in this study was approved by the Institutional Animal Care and Use Committee at the National University of Entre Rios and the Italian University Institute of Rosario (Rosario, Argentina; protocol N°028/12).

### 2.3. Histology and Histopathological Assessment

The excised liver samples ( $n = 4$ ) were immediately fixed in 4% glutaraldehyde (Electron Microscopy Sciences, Hatfield, PA, USA) in a phosphate-buffered saline solution (PBS 0.1 M, pH 7.2, 4 °C) and were post fixed in osmium tetroxide (1% in PBS) for 2 h. The samples were dehydrated through a graded ethanol series, placed in propylene oxide, and embedded in Epon-Araldite (Araldite 502/Embed 812, Electron Microscopy Sciences). Longitudinal serial semithin sections of 1  $\mu\text{m}$ , obtained using a Leica UltraCut UCT (Leica Microsystems, Wetzlar, Germany), were mounted on glass slides, stained with toluidine blue, and observed under an LM Leitz Dialux 20 E.B. (Leica Microsystems, Wetzlar, Germany), which was equipped with a digital camera.

The prevalence of each histological alteration was obtained by calculating the ratio between the number of fish affected by a specific alteration and the total number of fish. We also determined the histological changes' severity using a semi-quantitative method, which was conducted according to the data from the previous literature [51,52]. Briefly, the alterations were attributed to a specific reaction pattern (circulatory disturbances, regressive changes, progressive changes, and inflammation). Then, an importance factor was assigned to each observed alteration following the relevance of the change and its pathological importance (from 1, i.e., minimal pathological importance to 3, i.e., marked pathological importance). A score value was then assigned based on the degree and extent of each lesion as follows: 0 (unchanged), 2 (mild occurrence), 4 (moderate occurrence), and 6 (severe occurrence) (Table S2). The organ index ( $I_{\text{org}}$ ), representing the degree of organ damage, was calculated using the importance factor and the score value according to the following formula:

$$I_{\text{org}} = \sum_{\text{rp}} \sum_{\text{alt}} (a_{\text{org rp alt}} \times w_{\text{org rp alt}})$$

where org = organ, rp = reaction pattern, alt = alteration, a = score value, and w = importance factor.

### 2.4. Lipid Droplet Content

Lipid droplet analysis was performed on semithin sections (toluidine blue-stained). Four liver sections were photographed (100 $\times$ ) for each animal of both the control and Pb-exposed groups ( $n = 4$ ), and the percentage of area occupied by lipid droplets was measured. The lipid granules were isolated in each micrograph using the free and open-source ImageJ software (NIH, developed at the National Institutes of Health, a part of the U.S. Department of Health and Human Services), and the total area occupied by the granules was quantified.

The results, expressed as the percentage of area occupied by the lipid granules in each section, were statistically compared using two-way ANOVA followed by Tukey's multiple comparisons tests (at a significance level of 0.05). Data were checked for normality (Shapiro–Wilk test) and presented as the mean  $\pm$  standard deviation.

### 2.5. Quantitative Real-Time PCR

The excised liver samples of animals of both the treated and control groups ( $n = 6$ ) were promptly stored at  $-80\text{ }^{\circ}\text{C}$  for subsequent real-time PCR analyses. Total RNA was extracted using the PureLink RNA Mini Kit and the PureLink™ DNase Set (Thermo Fisher Scientific, Waltham, MA, USA) following the manufacturer's protocol. The quantity and quality of RNA were verified using a NanoDrop One spectrophotometer (Thermo Fisher Scientific, Waltham, MA, USA) and 1.5% agarose gel electrophoresis, respectively. We used  $2\text{ }\mu\text{g}$  of total RNA for the first-strand cDNA synthesis using the high-capacity RNA to cDNA kit (Applied Biosystems, Foster City, CA, USA); the resulting cDNA was kept at  $-20\text{ }^{\circ}\text{C}$ . The cDNA was used as a template for quantitative reverse transcription polymerase chain reaction (RT-qPCR) analysis to quantify the expression of metal regulatory transcription factor 1 (*mtf1*, NCBI Reference Sequence NM\_152981.1), superoxide dismutase 1 (*sod1*, NCBI Reference Sequence NM\_131294.1), and catalase (*cat*, NCBI Reference Sequence NM\_130912.2). RT-qPCR was performed in triplicate in a Light Cycler (Applied Biosystems StepOne, Real-Time PCR System, Foster City, CA, USA) using the TaqMan Gene Expression Assays (Thermo Fisher Scientific, Waltham, MA, USA). Each reaction contained  $2\text{ }\mu\text{L}$  of cDNA,  $10\text{ }\mu\text{L}$  of master mix (TaqMan Universal Master Mix II, Applied Biosystems),  $1\text{ }\mu\text{L}$  of assay mix (TaqMan Gene Expression Assay), and  $7\text{ }\mu\text{L}$  of RNase- and Dnase-free water, and was run according to the manufacturer's instructions: one cycle at  $50\text{ }^{\circ}\text{C}$  for 2 min,  $95\text{ }^{\circ}\text{C}$  for 10 min, 40 cycles at  $95\text{ }^{\circ}\text{C}$  for 15 s, and  $60\text{ }^{\circ}\text{C}$  for 1 min.

The glyceraldehyde-3-phosphate dehydrogenase (*gapdh*, NCBI Reference Sequence: NM\_001115114.1) and actin beta 1 (*actb1*, NCBI Reference Sequence: NM\_131031.2) genes were used as internal reference genes. The relative copy number of each analyzed gene was calculated according to the  $2^{-\Delta\Delta\text{CT}}$  comparative CT method.

## 3. Results

No mortality occurred during the whole experimental period, neither in the control nor in the exposed groups.

### 3.1. Control Group

The morphology of the *Danio rerio* liver is similar to that of other freshwater Teleosts [53,54], and only a brief description will be given in the present study. The parenchymal mass, even and compact, was crossed by a network of sinusoids surrounded by cords of hepatocytes (Figure 1a,b).

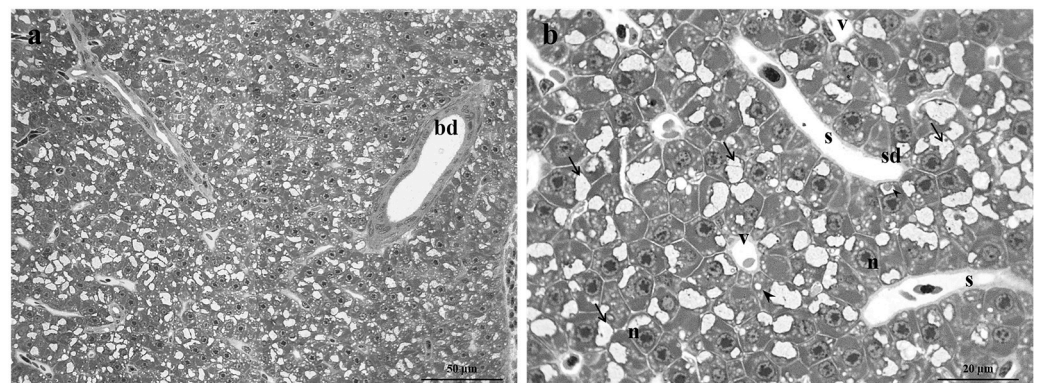


**Figure 1.** Light micrographs of the *Danio rerio* liver under basal conditions. (a) General organization of the liver parenchyma; note the bile ducts enclosed by the cuboidal epithelium. (b) High magnification showing the space of Disse between the hepatocytes and the sinusoid wall. Note the erythrocytes and a few macrophages in the lumen of the veins. Bd = bile duct, s = sinusoid, v = vein, n = nucleus, arrow = glycogen granules, arrowhead = lipid droplets, and sd = space of Disse.

The space of Disse is recognizable between the sinusoidal endothelium and the hepatocytes (Figure 1b). The veins bordered by a continuous endothelium were scattered within

the parenchyma; erythrocytes and a few macrophages could be detected in their lumen (Figure 1b). The bile ducts, lined by cuboidal epithelium, can be seen in the parenchyma (Figure 1a). Hepatocytes exhibit a polygonal shape with central spherical nuclei, numerous glycogen granules, and a few lipid droplets in their cytoplasm (Figure 1b).

### 3.2. Exposed Group

#### 3.2.1. Low Pb Concentration

After 48 h of exposure to the low Pb concentration, the overall morphological organization of the liver parenchyma was maintained (Class I normal organ structure, Table 1) (Figure 2a). However, the frequency of the bile duct degeneration and the congestion of blood vessels and sinusoids significantly increased compared to the control (Figure 2b,c and Figure 3a,b). An increase in lipid droplets in the hepatocyte cytoplasm was also recognizable (Figure 2c).

**Table 1.** Comparison in the organ index (mean  $\pm$  SD) between the control and Pb-exposed groups.

	2.5 $\mu\text{g/L}$ Pb	5 $\mu\text{g/L}$ Pb
CTRL	0.00 $\pm$ 0.00	0.00 $\pm$ 0.00
48 h	2.66 $\pm$ 1.15	16.00 $\pm$ 5.29 (a ***) (b **)
96 h	14.66 $\pm$ 3.05 (a **) (c *)	42.00 $\pm$ 2.40 (a ***) (b ***) (c ***)
192 h	35.33 $\pm$ 4.61 (a ***) (c ***)	53.33 $\pm$ 3.05 (a ***) (b ***) (c *)

Class I (index  $\leq 10$ ): normal organ structure; Class II (index 11–20): slight histological alterations; Class III (index 21–30): moderate histological alterations; Class IV (index 31–40): pronounced histological alterations of the organ; and Class V (index  $> 40$ ): severe histological alterations. a = significance of the low or high concentration groups with respect to the control group; b = significance of the high concentration group with respect to the low concentration group; c = significance of 96 h treatment with respect to 48 h treatment or 192 h treatment with respect to 96 h treatment. \*  $p \leq 0.05$ ; \*\*  $p \leq 0.01$ ; \*\*\*  $p = 0.001$ ; and \*\*\*\*  $p \leq 0.0001$ .

The extent and intensity of histological alterations increased after 96 h of exposure, becoming significantly higher compared to both the control and 48-h-exposed groups (Table 1), and their severity degree ranged from normal to slightly altered (Class II). The typical architecture of the bile ducts was no longer recognizable, and the cuboidal cells often showed signs of degeneration (Figure 2d). Moreover, detachment of the duct epithelium from connective tissue was frequently observed (Figures 2d and 3c). The lumen of some vessels and sinusoids was filled by a large number of blood cells and proliferating macrophages, which sporadically also migrated to the liver parenchyma (Figure 2e,f). Commonly observed hepatocyte abnormalities included cytoplasmic vacuolization, increased lipid droplets, and the emergence of the distinctive signs of apoptosis, such as deeply stained cytoplasm and degenerated nuclei (Figure 2e,f and Figure 3d–g). It was also observed that the occurrence of lysed areas was significantly higher than in the control and the 48-h-exposed groups (Figures 2g and 3h).

After 192 h of exposure, the architecture of the liver parenchyma was markedly compromised. The degrees of histopathological changes significantly increased compared to the control and 96-h-exposed groups (Class IV: pronounced histological alterations, Table 1). Hepatocyte cytoplasmic vacuolization, enhancement of lipid droplets, the appearance of extensive lysed areas, and congestion of vessels and sinusoids were frequently detected. However, their frequency did not differ from the 96-h-exposed group (Figure 3). In contrast, detachment of the bile duct epithelium dramatically increased, and macrophage proliferation, bile duct degeneration, pale necrotic hepatocytes, and dark colored apoptotic hepatocytes were observed in all samples (Figures 2h–j and 3a,c,f,g,i).

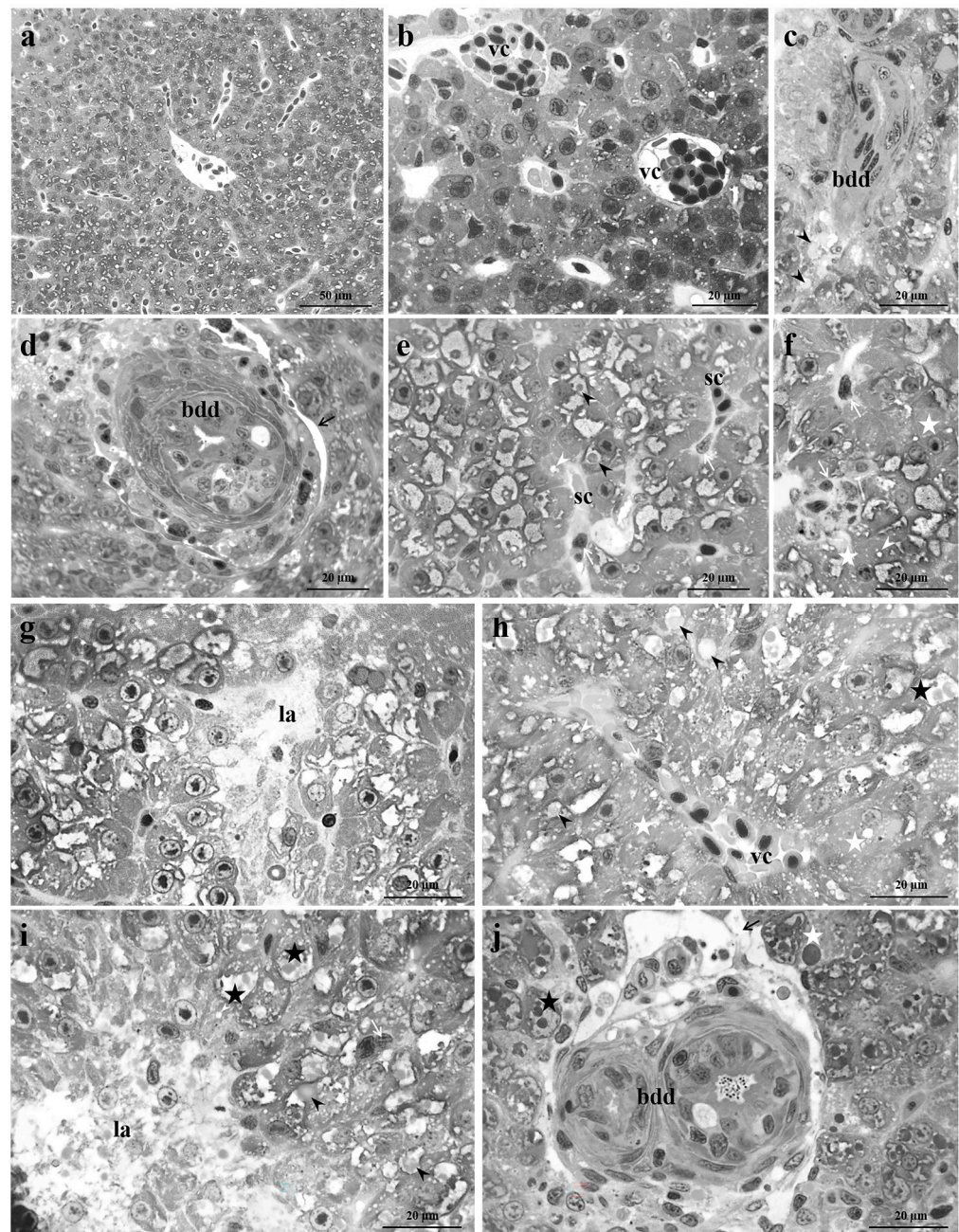


**Figure 2.** Light micrographs of *Danio rerio* liver after exposure to 2.5 µg/L of Pb. (a–c) After 48 h of exposure, bile duct degeneration and the congestion of blood vessels and sinusoids were observed. Note the increase in lipid droplet content. (d–g) After 96 h of exposure, the cuboidal epithelium lining the bile ducts was modified, and the detachment of the duct epithelium was evident. Note the congestion of blood vessels and sinusoids, macrophage proliferation, cytoplasmic vacuolization, the increase in lipid droplet content, and the appearance of both apoptotic and necrotic hepatocytes. Additionally, lysed areas were frequently observed. (h–j) After 192 h of exposure, cytoplasm vacuolization, the congestion of vessels and sinusoids, and numerous lipid droplets were frequently detected. Note the detachment of the bile duct epithelium, macrophage proliferation, and both apoptotic and necrotic hepatocytes. bdd = bile duct degeneration, vc = vessel congestion, sc = sinusoids congestion, black arrow = bile duct epithelial detachment, black arrowhead = lipid droplets, white arrowhead = cytoplasmic vacuolization, white arrow = macrophages proliferation, white star = apoptotic cell, black star = necrotic cell, and la = lysed area.

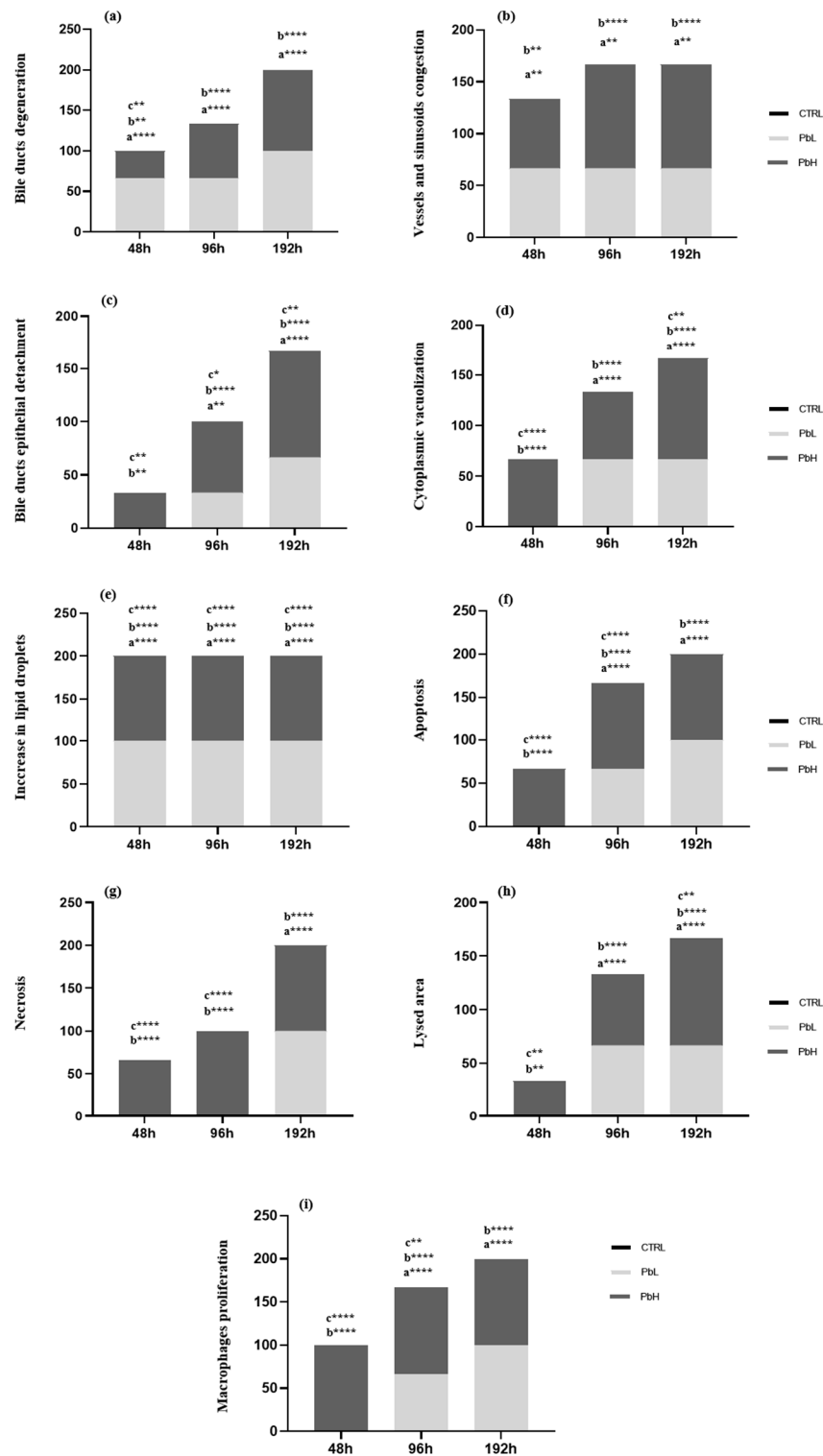


**Figure 3.** (a–i) Prevalence of the histological alterations in *Danio rerio* liver after exposure to 2.5 and 5 µg/L of Pb for 48, 96, and 192 h. <sup>a</sup>=significance in the low concentration group with respect to the control group. <sup>b</sup>=significance in the high concentration group with respect to the control group. <sup>c</sup>=significance of the high concentration group with respect to the low concentration group. \*  $p \leq 0.05$ ; \*\*  $p \leq 0.005$ ; and \*\*\*\*  $p \leq 0.0001$ .



### 3.2.2. High Pb Concentration

After 48 h of exposure to the high Pb concentration, the extent and intensity of histological alterations significantly increased compared to the control group (Class II slight histological alterations, Table 1). All morphological alterations observed in low-Pb-exposed groups precociously appeared (Figures 3a–i and 4a–c). Degeneration of the bile ducts, bile duct epithelial detachment, an increase in lipid droplets in hepatocyte cytoplasm, and the appearance of lysed areas were observed at a significantly higher frequency than in the control group (Figure 3a,c,e,h and Figure 4a,c).

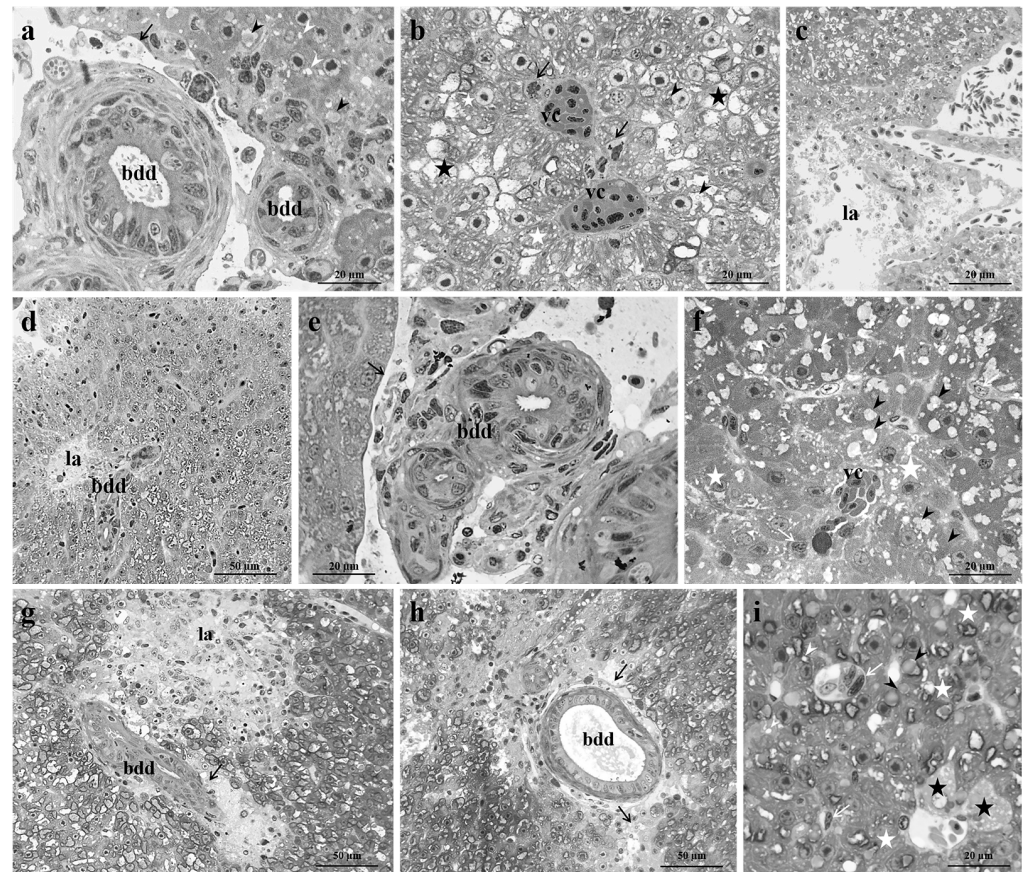


**Figure 4.** Light micrographs of *Danio rerio* liver after exposure to 5 µg/L of Pb. (a–c) After 48 h of exposure, bile duct degeneration, bile duct epithelial detachment, wide lysed areas, and numerous lipid droplets could be detected. Moreover, the vacuolization of hepatocyte cytoplasm, the congestion of blood vessels, and both apoptotic and necrotic cells were frequently visible. Note the proliferation of macrophages. (d–f) After 96 h of exposure, numerous degenerations, such as vessel and sinusoid congestion, macrophage proliferation, and apoptotic hepatocytes, were visible in all samples. Additionally, the increase in lipid content, cytoplasmic vacuolization, bile duct degeneration, detachment of the bile duct epithelium, and lysed areas were frequently detected. (g–i) After 192 h of exposure, all the considered alterations were detected in all samples. bdd = bile duct degeneration, vc = vessel congestion, sc = sinusoids congestion, black arrow = bile duct epithelial detachment, black arrowhead = lipid droplets, white arrowhead = cytoplasmic vacuolization, white arrow = macrophages proliferation, white star = apoptotic cell, black star = necrotic cell, and la = lysed area.

The incidence of cytoplasmic vacuolization, blood vessel congestion, as well as apoptotic and necrotic hepatocytes was significantly increased compared to the control and the low Pb concentration group (Figure 3b,d,f,g and Figure 4a,b). Moreover, macrophage proliferation was detected in 100% of the samples (Figures 3i and 4b).

The tissue degeneration significantly increased as the exposure proceeded, and after 96 h of exposure, the extent and intensity of histological alterations were higher compared to the control and low Pb concentration groups (Class III severe histological modifications, Table 1). The frequency of cytoplasmic vacuolization, lysed areas, bile duct degeneration, and bile duct epithelial detachment was significantly higher compared to the control and 48-h-exposed groups (Figure 3a,c,d,h and Figure 4d,e). Numerous alterations, such as vessel and sinusoid congestion, macrophage proliferation, and apoptotic hepatocytes, were detected in 100% of samples (Figure 3b,f,i and Figure 4f). Moreover, an increase in lipid droplet content was evident (Figure 3e,f).

The liver structure markedly changed after 192 h of exposure. The extent and intensity of histological alterations reached a peak and were statistically significant compared to the control and all treated groups (Class V severe histological alterations, Table 1). All the considered alterations were detected with an incidence of 100% (Figure 3a–i). Bile ducts displayed a severely modified architecture (Figure 4g,h). The lumen of vessels and sinusoids was filled with macrophages that frequently migrated in the liver parenchyma (Figure 4i). Hepatic dyschromia was more evident due to the increase in the numbers of both necrotic and apoptotic hepatocytes (Figure 4i). Cytoplasmic vacuolization and the growth of lipid droplets were prominent (Figure 4i).

### 3.3. Lipid Droplet Content

The lipid droplet amount, expressed as the percentage of the section area occupied by lipid droplets, showed a statistically significant difference in the Pb-exposed groups compared to the control. The lipid droplet content significantly increased after exposure to both tested concentrations at all time points (Figure 5). In more detail, the increase was significant after 48 h and became highly significant as the exposure proceeded; a significant difference could also be noted between the low and high exposure groups (Figure 5).

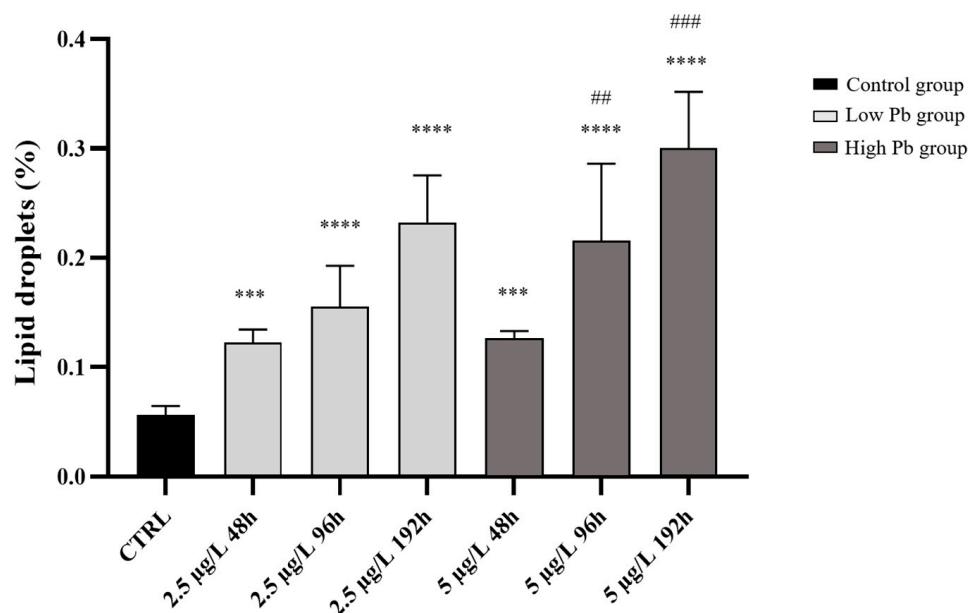


**Figure 5.** Percentage of the area occupied by lipid droplets in *Danio rerio* liver after exposure to 2.5 and 5 µg/L of Pb for 48, 96, and 192 h. Graphs indicate the mean ± S.D. Asterisks indicate significant differences between the treated and control groups. Hashtags indicate significant differences between the high Pb concentration group and the low Pb concentration group. \*\*\*  $p \leq 0.001$ ; \*\*\*\*  $p \leq 0.0001$ ; ##  $p \leq 0.005$ ; and ###  $p \leq 0.001$ .

### 3.4. Gene Expression

Metallothioneins (*mtf1*)—Exposure to the low Pb concentration induced a significant upregulation of *mtf1* compared to the control, starting from 96 h of exposure and peaking

after 192 h (Figure 6a). Highly significant upregulation was observed at 48 and 96 h when the high Pb dose was administered. A significant difference was detected between low and high concentration groups at these time points. The expression level decreased after 192 h, remaining significantly higher than the control (Figure 6a).

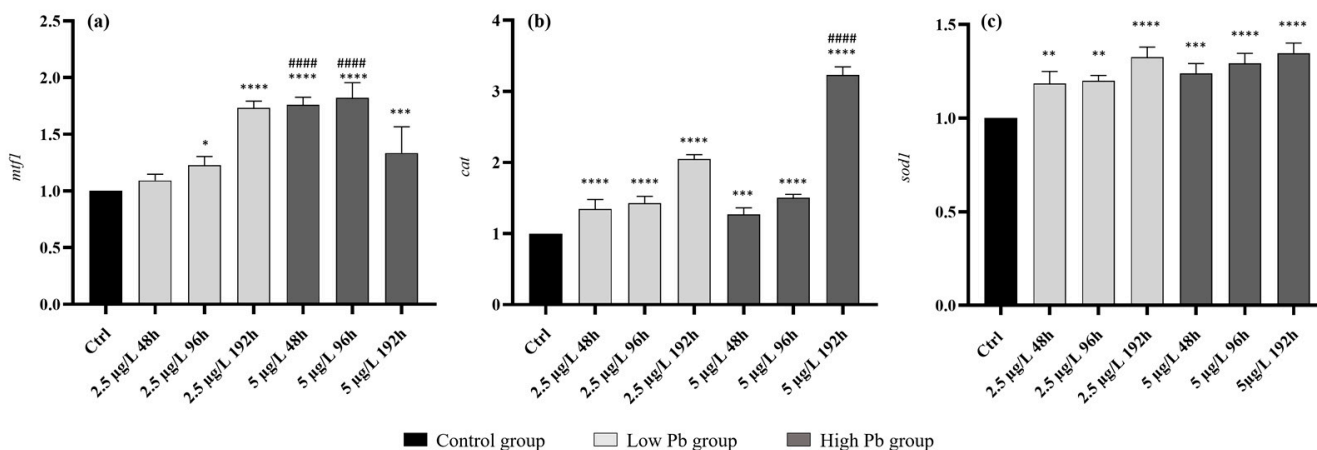


**Figure 6.** Gene expression in *Danio rerio* liver after exposure to 2.5 and 5 µg/L of Pb for 48, 96, and 192 h. Graphs indicate the mean ± S.D. (a) Metallothioneins (*mtfl*), (b) catalase (*cat*), and (c) superoxide dismutase (*sod1*). Asterisks indicate the significant differences between the treated and control groups. Hashtags indicate the significant differences between the high concentration and the low concentration groups. \*  $p \leq 0.05$ ; \*\*  $p \leq 0.005$ ; \*\*\*  $p \leq 0.001$ ; \*\*\*\*  $p \leq 0.0001$ ; #####  $p \leq 0.0001$ .

**Catalase (*cat*)**—After exposure to the low Pb concentration, a significant increase in *cat* expression was detected at all time points compared to the control, and the maximum level was reached after 192 h (Figure 6b). A similar transcriptional response was detected after exposure to a high Pb concentration. The highest expression level was noted after 192 h, which is when the upregulation was also significantly higher compared to the low-Pb-exposed groups (Figure 6b).

**Superoxide dismutase (*sod1*)**—Exposure to the low Pb concentration induced a significant upregulation of *sod1* at all time points compared to the control, peaking after 192 h. A similar pattern was detected when the high Pb dose was administered (Figure 6c).

#### 4. Discussion

Extensive data from the literature demonstrate that heavy metals must be recognized as priority pollutants due to their pervasive and persistent distribution in all environmental compartments [1–3,55]. Pb is highly toxic and non-biodegradable, and it is widely acknowledged as one of the most dangerous heavy metals for living organisms [8,9,56,57].

Information on the effects of naturally occurring Pb concentrations is mandatory for environmental and public safety in order to effectively assess the presumed harmful outcomes. However, most of the information about Pb toxicity in fish comes from studies on high Pb concentrations, which are not representative of naturally occurring contamination events. The number of studies explicitly assessing the impact of low Pb concentrations on fish species is extremely low.

Since the liver is responsible for many vital functions, including the accumulation and detoxification of pollutants [58], pathological alterations of this organ may easily interfere with the functioning of all physiological processes. Moreover, the liver of teleost fish is an organ widely used as a biomarker for fish health assessment because the effects of pollutant exposure can be evident at its cellular and tissue level [59,60].

##### 4.1. Morphological Modifications

In the present study, we demonstrated, for the first time, that exposure to two very low Pb concentrations induces severe histopathological and functional changes in zebrafish

liver. As revealed by our semi-quantitative analyses, the severity of injuries was time- and dose-dependent. Indeed, an evident pathological progression could be seen as the experiment proceeded in both experimental groups, but alterations precociously arose in the group exposed to the high Pb dose, and they also showed a higher severity at all exposure times.

According to the previous reports on *Oreochromis niloticus* when chronically exposed to high Pb concentrations [33,61], the first and most frequent alteration observed in *D. rerio* liver was the congestion of blood vessels and sinusoids. Such circulatory alterations have been regarded as reversible modifications that do not alter the normal function of the tissue [59], leading us to suppose that a recovery of the health status would be possible if the input of the toxicant ceased. In contrast, the inflammatory, regressive, and progressive changes that appeared or worsened starting from 96 h of exposure are non-reversible modifications that result in the complete loss of the liver parenchyma arrangement.

In our experiment, we also frequently observed the appearance of cytoplasmic vacuolizations, as has been previously reported, under both laboratory and field conditions in other freshwater species after exposure to Pb [62,63]. It has been suggested that hepatic vacuolations following exposure to heavy metals could be due to lipid and/or glycogen deposition, which are indicative of metabolic disorders [64]. Interestingly, a significant increase in lipid content and cytoplasmic vacuolizations was synchronously detected in all *D. rerio* samples exposed to Pb, thus suggesting that the appearance of vacuole structures could be related to lipid depositions. Our findings are, in general, in agreement with the data from the literature on rare minnows (*Gobiocypris rarus*) when they are subjected to acute waterborne cadmium exposure [65].

Another commonly observed phenomenon induced in zebrafish liver was the emergence of lysed areas, which is in agreement with the available reports on zebrafish liver after exposure to other heavy metals [54,66].

*D. rerio* also responded to Pb exposure by the proliferation of macrophages, which play a crucial role in regulating immune response, host protection, and tissue homeostasis [67]. Macrophage activation in fish is considered a bio-indicator of exposition to chemical contaminants, especially those associated with oxidative stress and lipid peroxidation [68,69].

Exposure to Pb affects ROS and reactive nitrogen species production through different mechanisms [21,70]. Whatever the pro-oxidant pathways, Pb triggers a cascade of oxidative reactions leading to protein unfolding, DNA/RNA damage, and the peroxidation of unsaturated lipids in cell membranes.

Among other heavy metals, Pb especially encourages iron-initiated membrane lipid oxidation in fish [21], which is considered an essential mediator of ferroptosis, a lytic form of regulated cell death (LRCD) [71]. Although nonmammalian vertebrates, including fish, exhibit such an oxidation pathway, the extent to which ferroptosis *per se* is involved is still poorly understood [72]. Metal-induced ferroptosis has been recently suggested in Japanese flounder that have been exposed to nickel and cobalt [73], as demonstrated by the enhancement of ferroptosis-related pathways, simultaneous cell swelling, and the cytoplasmic depletion in hepatocytes.

Different types of cell death may coexist in the Pb-induced pathological context, including lytic forms of hepatocellular death, such as ferroptosis, which share morphologic features with passive necrosis [74]. In our study, we clearly showed the concurrent presence of dark-stained hepatocytes (which represent the apoptotic cell population), and pale and swollen hepatocytes (which might belong to necrotic or ferroptotic cells). Therefore, based on the histological results and the significant upregulation of antioxidant enzymes (see below), we speculated that ferroptosis may be a key regulator of Pb-induced liver injury.

#### 4.2. Gene Expression

Superoxide dismutase (SOD) and catalase (CAT)—In fish, the first antioxidant response against elevated ROS levels is the modulation of key enzymes, including superoxide

dismutase (SOD) and catalase (CAT), which are two major antioxidant enzymes and good indicators of oxidative stress [75,76].

Here, we clearly showed a significant upregulation of such enzymes after exposure to both Pb concentrations at all time points. SOD and CAT modulation induced by Pb in fish liver has been investigated in several species, with contradictory results, as both the upregulation and downregulation of these enzymes have been reported [17,21,41,77,78]. In zebrafish liver, Wang and colleagues [41] recently demonstrated that chronic exposure to high Pb concentrations resulted in an initial increased activity of SOD and CAT (45 days), followed by a reduction when the experiment was prolonged (90 days). They suggested that the excess ROS may exhaust the antioxidant system, explaining the reversing trend in SOD and CAT activity. It must be emphasized that a direct comparison of our results with the literature data is difficult since available information is limited to the effects induced by high Pb concentrations and/or deals with chronic exposure assays. More studies are needed to understand the physiological and molecular mechanisms underlying the modulation of antioxidant enzymes after Pb exposure to low and realistic environmental concentrations.

Metallothioneins (MTs)—MTs are recognized as sensitive biomarkers of heavy metal exposure in aquatic organisms. They play an important role in maintaining redox potentials, essential metals homeostasis, and detoxifying non-essential metals [45]. Under basal conditions, MTs are expressed in the fish's liver, but their increase is strictly related to metal exposure [49].

An increase in MT expression has been demonstrated in the liver of both marine and freshwater fish after dietary exposure to Pb, and in fish coming from Pb-contaminated areas [49,79]. Furthermore, our recent study reported an increase in the expression of *mtf1* in zebrafish gills after Pb exposure [25]. Although MT induction has been demonstrated in several fish organs after exposure to heavy metals, the liver is one of the organs that first responds to the toxic input [79]. Accordingly, we confirm here the use of the liver as a sensitive organ through which to investigate early exposure to Pb and the importance of using MTs as valuable biomarkers. We demonstrated an upregulation of metallothionein, starting from 96 h of exposure to the low concentration of Pb, while the overexpression was precocious (from 48 h) when the high dose of the contaminant is administered.

## 5. Conclusions

Overall, the data presented here clearly show that short-term exposure to two very low and naturally occurring concentrations of Pb is associated with significant histological alterations in the *Danio rerio* liver. Our semi-quantitative morphological evaluation shows that the severity and extent of injuries increase with dose and exposure time, resulting in irreversible histological changes at the end of exposure to the high tested concentration. We also demonstrated that Pb administration induces metabolic disorders, and this is evident in the significant increase in lipid content in all exposed groups.

Our results confirm that the production of reactive oxygen species is an essential mechanism of Pb toxicity in the liver, thereby leading to an upregulation of the antioxidant enzymes (*sod* and *cat*). These results confirm MT upregulation to be a powerful marker of lead contamination.

**Supplementary Materials:** The following supporting information can be downloaded at: <https://www.mdpi.com/article/10.3390/fishes8070342/s1>, Table S1: Detected Pb concentrations in the control group and exposure solutions; Table S2: Histopathological changes observed in *Danio rerio* liver.

**Author Contributions:** Methodology, R.M., V.C., E.P. and L.O.; investigation, R.M., V.C. and E.B.; formal analysis, A.I.M.A., F.T., L.O. and M.M.; data curation, F.T. and S.S.; software, A.I.M.A., F.T. and S.S.; writing—original draft preparation, R.M., V.C. and E.B.; writing—review and editing, E.B.; project administration, E.B. All authors have read and agreed to the published version of the manuscript.

**Funding:** This research did not receive any specific grant from funding agencies in the public, commercial, or not-for-profit sectors.

**Institutional Review Board Statement:** The use of animals in this study was approved by the Institutional Animal Care and Use Committee at the National University of Entre Rios and the Italian University Institute of Rosario (Rosario, Argentina; protocol N. 028/12).

**Data Availability Statement:** The data presented in this study are available on request from the corresponding authors.

**Conflicts of Interest:** The authors declare no conflict of interest.

## References

- Kortei, N.K.; Heymann, M.E.; Essuman, E.K.; Kpodo, F.M.; Akonor, P.T.; Lokpo, S.Y.; Boadi, N.O.; Ayim-Akonor, M.; Tettey, C. Health risk assessment and levels of toxic metals in fishes (*Oreochromis niloticus* and *Clarias anguillaris*) from Ankobrah and Pra basins: Impact of illegal mining activities on food safety. *Toxicol. Rep.* **2020**, *7*, 360–369. [CrossRef]
- Chen, G.W.; Lee, D.Y.; Chen, P.J. Use of embedded Chelex chelating resin and sediment toxicity bioassays with medaka embryos to determine the bioavailability and toxicity of lead-contaminated sediment. *Sci. Total Environ.* **2020**, *745*, 140794. [CrossRef] [PubMed]
- Ezemonye, L.I.; Adebayo, P.O.; Enuneku, A.A.; Tongo, I.; Ogbomida, E. Potential health risk consequences of heavy metal concentrations in surface water, shrimp (*Macrobrachium macrobrachion*) and fish (*Brycinus longipinnis*) from Benin River, Nigeria. *Toxicol. Rep.* **2019**, *6*, 1–9. [CrossRef] [PubMed]
- Bansod, B.; Kumar, T.; Thakur, R.; Rana, S.; Singh, I. A review on various electrochemical techniques for heavy metal ions detection with different sensing platforms. *Biosens. Bioelectron.* **2017**, *94*, 443–455. [CrossRef]
- Brunelli, E.; Mauceri, A.; Maisano, M.; Bernabò, I.; Giannetto, A.; de Domenico, E.; Corapi, B.; Tripepi, S.; Fasulo, S. Ultrastructural and immunohistochemical investigation on the gills of the teleost, *Thalassoma pavo* L., exposed to cadmium. *Acta Histochem.* **2011**, *113*, 201–213. [CrossRef] [PubMed]
- Cai, L.M.; Wang, Q.S.; Luo, J.; Chen, L.G.; Zhu, R.L.; Wang, S.; Tang, C.H. Heavy metal contamination and health risk assessment for children near a large Cu-smelter in central China. *Sci. Total Environ.* **2019**, *650*, 725–733. [CrossRef]
- Cheema, A.I.; Liu, G.; Yousaf, B.; Abbas, Q.; Zhou, H. A comprehensive review of biogeochemical distribution and fractionation of lead isotopes for source tracing in distinct interactive environmental compartments. *Sci. Total Environ.* **2020**, *719*, 135658. [CrossRef]
- Shi, L.; Wang, N.; Hu, X.; Yin, D.; Wu, C.; Liang, H.; Cao, W.; Cao, H. Acute toxic effects of lead (Pb<sup>2+</sup>) exposure to rare minnow (*Gobiocypris rarus*) revealed by histopathological examination and transcriptome analysis. *Environ. Toxicol. Pharmacol.* **2020**, *78*, 103385. [CrossRef]
- Kumar, A.; Kumar, A.; MMS, C.P.; Chaturvedi, A.K.; Shabnam, A.A.; Subrahmanyam, G.; Mondal, R.; Gupta, D.K.; Malyan, S.K.; Kumar, S.S.; et al. Lead toxicity: Health hazards, influence on food chain, and sustainable remediation approaches. *Int. J. Environ. Res. Public Health* **2020**, *17*, 2179. [CrossRef]
- United States Environmental Protection Agency, “Learn About Lead”. EPA. 2022. Available online: <https://www.epa.gov/lead/learn-about-lead> (accessed on 2 April 2023).
- Bashir, I.; Lone, F.A.; Bhat, R.A.; Mir, S.A.; Dar, Z.A.; Dar, S.A. Concerns and threats of contamination on aquatic ecosystems. In *Bioremediation and Biotechnology*; Hakeem, K., Bhat, R., Qadri, H., Eds.; Springer: Cham, Switzerland, 2020; pp. 1–26. [CrossRef]
- Su, G.; Logez, M.; Xu, J.; Tao, S.; Villéger, S.; Brosse, S. Human impacts on global freshwater fish biodiversity. *Science* **2021**, *371*, 835–838. [CrossRef]
- Keke, U.N.; Mgbemena, A.S.; Arimoro, F.O.; Omalu, I.C. Biomonitoring of effects and accumulations of heavy metals insults using some helminth parasites of fish as bio-indicators in an Afrotropical stream. *Front. Environ. Sci.* **2020**, *8*, 576080. [CrossRef]
- Łuczyńska, J.; Paszczyk, B.; Łuczyński, M.J. Fish as a bioindicator of heavy metals pollution in aquatic ecosystem of Pluszne Lake, Poland, and risk assessment for consumer’s health. *Ecotoxicol. Environ. Saf.* **2018**, *153*, 60–67. [CrossRef] [PubMed]
- Macirella, R.; Brunelli, E. Morphofunctional alterations in zebrafish (*Danio rerio*) gills after exposure to mercury chloride. *Int. J. Mol. Med. Sci.* **2017**, *18*, 824. [CrossRef]
- Paul, S.; Mandal, A.; Bhattacharjee, P.; Chakraborty, S.; Paul, R.; Mukhopadhyay, B.K. Evaluation of water quality and toxicity after exposure of lead nitrate in fresh water fish, major source of water pollution. *Egypt. J. Aquat. Res.* **2019**, *45*, 345–351. [CrossRef]
- Dai, J.; Zhang, L.; Du, X.; Zhang, P.; Li, W.; Guo, X.; Li, Y. Effect of lead on antioxidant ability and immune responses of *Crucian carp*. *Biol. Trace Elem. Res.* **2018**, *186*, 546–553. [CrossRef] [PubMed]
- Zhao, L.; Zheng, Y.G.; Feng, Y.H.; Li, M.Y.; Wang, G.Q.; Ma, Y.F. Toxic effects of waterborne lead (Pb) on bioaccumulation, serum biochemistry, oxidative stress and heat shock protein-related genes expression in *Channa argus*. *Chemosphere* **2020**, *261*, 127714. [CrossRef] [PubMed]
- Ishaque, A.; Ishaque, S.; Arif, A.; Abbas, H.G. Toxic effects of lead on fish and human. *Biol. Clin. Sci. Res. J.* **2020**, *2020*, e045. [CrossRef]

20. Jing, H.; Zhang, Q.; Li, S.; Gao, X.J. Pb exposure triggers MAPK-dependent inflammation by activating oxidative stress and miRNA-155 expression in carp head kidney. *Fish Shellfish Immunol.* **2020**, *106*, 219–227. [[CrossRef](#)]
21. Lee, J.W.; Choi, H.; Hwang, U.K.; Kang, J.C.; Kang, Y.J.; Kim, K.I.; Kim, J.H. Toxic effects of lead exposure on bioaccumulation, oxidative stress, neurotoxicity, and immune responses in fish: A review. *Environ. Toxicol. Pharmacol.* **2019**, *68*, 101–108. [[CrossRef](#)] [[PubMed](#)]
22. Paul, N.; Chakraborty, S.; Sengupta, M. Lead toxicity on non-specific immune mechanisms of freshwater fish *Channa punctatus*. *Aquat. Toxicol.* **2014**, *152*, 105–112. [[CrossRef](#)]
23. Al-Balawi, H.F.A.; Al-Akel, A.S.; Al-Misned, F.; Suliman, E.A.M.; Al-Ghanim, K.A.; Mahboob, S.; Ahmad, Z. Effects of sub-lethal exposure of lead acetate on histopathology of gills, liver, kidney and muscle and its accumulation in these organs of *Clarias gariepinus*. *Braz. Arch. Biol. Technol.* **2013**, *56*, 293–302. [[CrossRef](#)]
24. Macirella, R.; Sesti, S.; Bernabò, I.; Tripepi, M.; Godbert, N.; Brunelli, E. Lead toxicity in seawater teleosts: A morphofunctional and ultrastructural study on the gills of the Ornate wrasse (*Thalassoma pavo* L.). *Aquat. Toxicol.* **2019**, *211*, 193–201. [[CrossRef](#)] [[PubMed](#)]
25. Curcio, V.; Macirella, R.; Sesti, S.; Ahmed, A.I.; Talarico, F.; Tagarelli, A.; Mezzasalma, M.; Brunelli, E. Morphological and functional alterations induced by two ecologically relevant concentrations of Lead on *Danio rerio* gills. *Int. J. Mol. Sci.* **2022**, *23*, 9165. [[CrossRef](#)] [[PubMed](#)]
26. Zhai, Q.; Wang, H.; Tian, F.; Zhao, J.; Zhang, H.; Chen, W. Dietary *Lactobacillus plantarum* supplementation decreases tissue lead accumulation and alleviates lead toxicity in Nile tilapia (*Oreochromis niloticus*). *Aquacult. Res.* **2017**, *48*, 5094–5103. [[CrossRef](#)]
27. Bawuro, A.A.; Voegborlo, R.B.; Adimado, A.A. Bioaccumulation of heavy metals in some tissues of fish in Lake Geriyo, Adamawa State, Nigeria. *J. Environ. Public Health* **2018**, *2018*, 1854892. [[CrossRef](#)]
28. Tanhan, P.; Imsilp, K.; Lansubsakul, N.; Thong-asa, W. Oxidative response to Cd and Pb accumulation in coastal fishes of Pattani Bay. *Ital. J. Anim. Sci.* **2023**, *22*, 148–156. [[CrossRef](#)]
29. Kumar, E.K.; Midhun, S.J.; Vysakh, A.; James, T.J. Antagonistic effects of dietary *Moringa oleifera* on hemato-biochemical and oxidative stress of lead nitrate intoxicated Nile tilapia, *Oreochromis niloticus*. *Aquacult. Res.* **2021**, *52*, 6164–6178. [[CrossRef](#)]
30. Eroglu, A.; Dogan, Z.; Kanak, E.G.; Atli, G.; Canli, M. Effects of heavy metals (Cd, Cu, Cr, Pb, Zn) on fish glutathione metabolism. *Environ. Sci. Pollut. Res.* **2015**, *22*, 3229–3237. [[CrossRef](#)]
31. Rajamanickam, D.; Devadason, C.G. Histopathological alterations in gill, liver, and brain of Nile Tilapia (*Oreochromis Niloticus*), exposed to Lead Nitrate (Pb [NO<sub>3</sub>]<sub>2</sub>). *Int. J. Sci. Technol. Res.* **2021**, *3*, 149–153.
32. Mustafa, S.A.; Al-Faragi, J.K.; Salman, N.M.; Al-Rudainy, A.J. Histopathological alterations in gills, liver and kidney of common carp, *Cyprinus carpio* exposed to lead Acetate. *Adv. Anim. Vet. Sci.* **2017**, *5*, 371–376.
33. Doaa, M.M.; Hanan, H.A. Histological changes in selected organs of *Oreochromis niloticus* exposed to doses of lead acetate. *J. Life Sci. Biomed.* **2013**, *3*, 256–263.
34. Abdel-Warith, A.W.A.; Younis, E.S.M.; Al-Asgah, N.A.; Rady, A.M.; Allam, H.Y. Bioaccumulation of lead nitrate in tissues and its effects on hematological and biochemical parameters of *Clarias gariepinus*. *Saudi J. Biol. Sci.* **2020**, *27*, 840–845. [[CrossRef](#)] [[PubMed](#)]
35. Li, X.; Zhang, B.; Li, N.; Ji, X.; Liu, K.; Jin, M. Zebrafish neurobehavioral phenomics applied as the behavioral warning methods for fingerprinting endocrine disrupting effect by lead exposure at environmentally relevant level. *Chemosphere* **2019**, *231*, 315–325. [[CrossRef](#)]
36. Curcio, V.; Macirella, R.; Sesti, S.; Ahmed, A.I.; Talarico, F.; Pizzolotto, R.; Tagarelli, A.; Mezzasalma, M.; Brunelli, E. The role of exposure window and dose in determining lead toxicity in developing Zebrafish. *Chemosphere* **2022**, *307*, 136095. [[CrossRef](#)]
37. Lei, P.; Zhang, W.; Ma, J.; Xia, Y.; Yu, H.; Du, J.; Fang, Y.; Wang, L.; Zhang, K.; Jin, L.; et al. Advances in the utilization of Zebrafish for assessing and understanding the mechanisms of Nano-/Microparticles toxicity in water. *Toxics* **2023**, *11*, 380. [[CrossRef](#)]
38. Magyary, I. Recent advances and future trends in zebrafish bioassays for aquatic ecotoxicology. *Ecocycles* **2018**, *4*, 12–18. [[CrossRef](#)]
39. Zhang, H.; Liu, Y.; Liu, R.; Liu, C.; Chen, Y. Molecular mechanism of lead-induced superoxide dismutase inactivation in zebrafish livers. *J. Phys. Chem. B* **2014**, *118*, 14820–14826. [[CrossRef](#)]
40. Xia, J.; Lu, L.; Jin, C.; Wang, S.; Zhou, J.; Ni, Y.; Zhengwei, F.; Jin, Y. Effects of short-term lead exposure on gut microbiota and hepatic metabolism in adult zebrafish. *Comp. Biochem. Physiol. Part C Toxicol. Pharmacol.* **2018**, *209*, 1–8. [[CrossRef](#)]
41. Wang, G.; Wang, T.; Zhang, X.; Chen, J.; Feng, C.; Yun, S.; Cheng, Y.; Cheng, F.; Cao, J. Sex-specific effects of fluoride and lead exposures on histology, antioxidant physiology, and immune system in the liver of zebrafish (*Danio rerio*). *Ecotoxicology* **2022**, *31*, 396–414. [[CrossRef](#)]
42. Shah, Z.U.; Parveen, S. Oxidative, biochemical and histopathological alterations in fishes from pesticide contaminated river Ganga, India. *Sci. Rep.* **2022**, *12*, 3628. [[CrossRef](#)]
43. Opute, P.A.; Oboh, I.P. Hepatotoxic effects of atrazine on *Clarias gariepinus* (Burchell, 1822): Biochemical and histopathological studies. *Arch. Environ. Contam. Toxicol.* **2021**, *80*, 414–425. [[CrossRef](#)] [[PubMed](#)]
44. Bakıu, R.; Pacchini, S.; Piva, E.; Schumann, S.; Tolomeo, A.M.; Ferro, D.; Irato, P.; Santovito, G. Metallothionein expression as a physiological response against metal toxicity in the striped rockcod *Trematomus hansonii*. *Int. J. Mol. Sci.* **2022**, *23*, 12799. [[CrossRef](#)]
45. Wang, W.C.; Mao, H.; Ma, D.D.; Yang, W.X. Characteristics, functions, and applications of metallothionein in aquatic vertebrates. *Front. Mar. Sci.* **2014**, *1*, 34. [[CrossRef](#)]

46. Hauser-Davis, R.A. The current knowledge gap on metallothionein mediated metal-detoxification in Elasmobranchs. *PeerJ* **2020**, *8*, e10293. [[CrossRef](#)]
47. Yin, J.; Wang, A.P.; Li, W.F.; Shi, R.; Jin, H.T.; Wei, J.F. Sensitive biomarkers identification for differentiating Cd and Pb induced toxicity on zebrafish embryos. *Environ. Toxicol. Pharm.* **2017**, *56*, 340–349. [[CrossRef](#)] [[PubMed](#)]
48. Maiti, A.K.; Saha, N.C.; Paul, G. Effect of lead on oxidative stress, Na<sup>+</sup>K<sup>+</sup>ATPase activity and mitochondrial electron transport chain activity of the brain of *Clarias batrachus* L. *Bull. Environ. Contam. Toxicol.* **2010**, *84*, 672–676. [[CrossRef](#)]
49. Kim, J.H.; Kang, J.C. Effects of sub-chronic exposure to lead (Pb) and ascorbic acid in juvenile rockfish: Antioxidant responses, MT gene expression, and neurotransmitters. *Chemosphere* **2017**, *171*, 520–527. [[CrossRef](#)]
50. Morcillo, P.; Esteban, M.Á.; Cuesta, A. Heavy metals produce toxicity, oxidative stress and apoptosis in the marine teleost fish SAF-1 cell line. *Chemosphere* **2016**, *144*, 225–233. [[CrossRef](#)] [[PubMed](#)]
51. Bernet, D.; Schmidt, H.; Meier, W.; Burkhardt-Holm, P.; Wahli, T. Histopathology in fish: Proposal for a protocol to assess aquatic pollution. *J. Fish Dis.* **1999**, *22*, 25–34. [[CrossRef](#)]
52. Santos, R.M.B.; Monteiro, S.M.V.; Cortes, R.M.V.; Pacheco, F.A.L.; Fernandes, L.F.S. Seasonal differences in water pollution and liver histopathology of Iberian barbel (*Luciobarbus bocagei*) and Douro nase (*Pseudochondrostoma durienne*) in an agricultural watershed. *Water* **2022**, *14*, 444. [[CrossRef](#)]
53. Macirella, R.; Curcio, V.; Ahmed, A.I.M.; Pellegrino, D.; Brunelli, E. Effect of short-term exposure to low concentration of tebuconazole: Morphological, histometric and functional modifications in *Danio rerio* liver. *Eur. Zool. J.* **2022**, *89*, 331–345. [[CrossRef](#)]
54. Macirella, R.; Guardia, A.; Pellegrino, D.; Bernabò, I.; Tronci, V.; Ebbesson, L.O.; Sesti, S.; Tripepi, S.; Brunelli, E. Effects of two sublethal concentrations of mercury chloride on the morphology and metallothionein activity in the liver of zebrafish (*Danio rerio*). *Int. J. Mol. Sci.* **2016**, *17*, 361. [[CrossRef](#)] [[PubMed](#)]
55. Bhat, R.A.; Bakhshalizadeh, S.; Guerrero, M.C.; Kesbiç, O.S.; Fazio, F. Toxic effect of heavy metals on ovarian deformities, apoptotic changes, oxidative stress, and steroid hormones in rainbow trout. *J. Trace Elem. Med. Biol.* **2023**, *75*, 127106. [[CrossRef](#)]
56. Ali, H.; Khan, E.; Ilahi, I. Environmental chemistry and ecotoxicology of hazardous heavy metals: Environmental persistence, toxicity, and bioaccumulation. *J. Chem.* **2019**, *2019*, 6730305. [[CrossRef](#)]
57. Bakhshalizadeh, S.; Mora-Medina, R.; Fazio, F.; Parrino, V.; Ayala-Soldado, N. Determination of the Heavy Metal Bioaccumulation Patterns in Muscles of Two Species of Mulletts from the Southern Caspian Sea. *Animals* **2022**, *12*, 2819. [[CrossRef](#)]
58. Agbohessi, P.; Olowo, L.; Degila, B.; Houedjissi, G.; Imorou Toko, I.; Mandiki, S.N.; Kestemont, P. Comparative assessment of acute toxicity and histological changes in liver of African catfish *Clarias gariepinus* exposed to cotton insecticides. *J. Environ. Sci. Health Part B* **2023**, *58*, 31–44. [[CrossRef](#)] [[PubMed](#)]
59. Agamy, E. Histopathological changes in the livers of rabbit fish (*Siganus canaliculatus*) following exposure to crude oil and dispersed oil. *Toxicol. Pathol.* **2012**, *40*, 1128–1140. [[CrossRef](#)]
60. Popović, N.T.; Čižmek, L.; Babić, S.; Strunjak-Perović, I.; Čož-Rakovac, R. Fish liver damage related to the wastewater treatment plant effluents. *Environ. Sci. Pollut. Res.* **2023**, *30*, 48739–48768. [[CrossRef](#)] [[PubMed](#)]
61. Khidr, B.M.; Mekkawy, I.A.; Harabawy, A.S.; Ohaida, A.S. Effect of lead nitrate on the liver of the cichlid fish (*Oreochromis niloticus*): A light microscope study. *PJBS* **2012**, *15*, 854–862. [[CrossRef](#)] [[PubMed](#)]
62. Rajeshkumar, S.; Liu, Y.; Ma, J.; Duan, H.Y.; Li, X. Effects of exposure to multiple heavy metals on biochemical and histopathological alterations in common carp, *Cyprinus carpio* L. *Fish Shellfish Immunol.* **2017**, *70*, 461–472. [[CrossRef](#)] [[PubMed](#)]
63. Shahid, S.; Sultana, T.; Sultana, S.; Hussain, B.; Irfan, M.; Al-Ghanim, K.A.; Misned, F.A.; Mahboob, S. Histopathological alterations in gills, liver, kidney and muscles of *Ictalurus punctatus* collected from pollutes areas of River. *Braz. J. Biol.* **2020**, *81*, 814–821. [[CrossRef](#)]
64. Abalaka, S.E. Heavy metals bioaccumulation and histopathological changes in *Auchenoglanis occidentalis* fish from Tiga dam, Nigeria. *J. Environ. Health Sci. Eng.* **2015**, *13*, 67. [[CrossRef](#)] [[PubMed](#)]
65. Liu, X.H.; Pang, X.; Jin, L.; Pu, D.Y.; Wang, Z.J.; Zhang, Y.G. Exposure to acute waterborne cadmium caused severe damage on lipid metabolism of freshwater fish, revealed by nuclear lipid droplet deposition in hepatocytes of rare minnow. *Aquat. Toxicol.* **2023**, *257*, 106433. [[CrossRef](#)]
66. Paris-Palacios, S.; Biagianti-Risbourg, S.; Vernet, G. Biochemical and (ultra) structural hepatic perturbations of *Brachydanio rerio* (Teleostei, Cyprinidae) exposed to two sublethal concentrations of copper sulfate. *Aquat. Toxicol.* **2000**, *50*, 109–124. [[CrossRef](#)]
67. Broeg, K. Acid phosphatase activity in liver macrophage aggregates as a marker for pollution-induced immunomodulation of the non-specific immune response in fish. *Helgol. Mar. Res.* **2003**, *57*, 166–175. [[CrossRef](#)]
68. Valdez Domingos, F.X.; Assis, H.C.S.; Silva, M.D.; Damian, R.C.; Almeida, A.I.M.; Cestari, M.M.; Randi, M.A.F.; Oliveira Ribeiro, C.A. Anthropogenic Impact Evaluation of Two Brazilian Estuaries Through Biomarkers in Fish. *J. Braz. Soc. Ecotoxicol.* **2009**, *4*, 21–30. [[CrossRef](#)]
69. Sinha, R. Macrophage: A Key Player of Teleost Immune System. In *Macrophages-140 Years of Their Discovery*; IntechOpen: London, UK, 2022. [[CrossRef](#)]
70. Curcio, V.; Macirella, R.; Sesti, S.; Pellegrino, D.; Ahmed, A.I.; Brunelli, E. Morphological and molecular alterations induced by lead in embryos and larvae of *Danio rerio*. *Appl. Sci.* **2021**, *11*, 7464. [[CrossRef](#)]
71. Xia, X.; He, B.; Zhang, X.; Cheng, Z.; Liu, M.; Wei, X.; Jiang, J.; Hu, J. Lytic regulated cell death in aquaculture fish. *Rev. Aquacult.* **2021**, *13*, 1549–1564. [[CrossRef](#)]



72. Conrad, M.; Kagan, V.E.; Bayir, H.; Pagnussat, G.C.; Head, B.; Traber, M.G.; Stockwell, B.R. Regulation of lipid peroxidation and ferroptosis in diverse species. *Genes Dev.* **2018**, *32*, 602–619. [[CrossRef](#)] [[PubMed](#)]
73. Sun, Z.; Gong, C.; Ren, J.; Zhang, X.; Wang, G.; Liu, Y.; Ren, Y.; Zhao, Y.; Yu, Q.; Wang, Y.; et al. Toxicity of nickel and cobalt in Japanese flounder. *Environ. Poll.* **2020**, *263*, 114516. [[CrossRef](#)] [[PubMed](#)]
74. Gautheron, J.; Gores, G.J.; Rodrigues, C.M. Lytic cell death in metabolic liver disease. *J. Hepatol.* **2020**, *73*, 394–408. [[CrossRef](#)] [[PubMed](#)]
75. Stephenie, S.; Chang, Y.P.; Gnanasekaran, A.; Esa, N.M.; Gnanaraj, C. An insight on superoxide dismutase (SOD) from plants for mammalian health enhancement. *J. Funct. Foods* **2020**, *68*, 103917. [[CrossRef](#)]
76. Shi, Q.; Xiong, X.; Wen, Z.; Qin, C.; Li, R.; Zhang, Z.; Gong, Q.; Wu, X. Cu/Zn Superoxide dismutase and catalase of Yangtze Sturgeon, *Acipenser dabryanus*: Molecular cloning, tissue distribution and response to fasting and refeeding. *Fishes* **2022**, *7*, 35. [[CrossRef](#)]
77. Alak, G.; Atamanalp, M.; Topal, A.; Arslan, H.; Kocaman, E.M.; Oruc, E. Effect of sub-lethal lead toxicity on the histopathological and antioxidant enzyme activity of rainbow trout (*Oncorhynchus mykiss*). *Fresenius Environ. Bull.* **2013**, *22*, 733–738.
78. Jing, D.; Li, M.; Zhang, Y.; Yuan, L.; Wang, R.; Gong, Y. Differential induction of enzymes and genes involved in oxidative stress in gill and liver tissues of mudskipper *Boleophthalmus pectinirostris* exposed to lead. *Turk. J. Fish. Aquat. Sci.* **2017**, *17*, 437–443. [[CrossRef](#)]
79. Girgis, S.M.; Mabrouk, D.M.; Hanna, M.I.; Abd ElRaouf, A. Seasonal assessment of some heavy metal pollution and Metallothionein gene expression in cultured *Oreochromis niloticus*. *Bull. Natl. Res. Cent.* **2019**, *43*, 131. [[CrossRef](#)]

**Disclaimer/Publisher’s Note:** The statements, opinions and data contained in all publications are solely those of the individual author(s) and contributor(s) and not of MDPI and/or the editor(s). MDPI and/or the editor(s) disclaim responsibility for any injury to people or property resulting from any ideas, methods, instructions or products referred to in the content.